JOURNAL OF MATERIALS SCIENCE 23 (1988) 2079–2086

Analysis of fatigue crack tip plasticity in Fe–2.6Si

YUCEL BIROL
Department of Materials Science and Engineering, Case Western Reserve University, Cleveland, Ohio 44106, USA

Surface roughness analysis, etch-pit, and recrystallization techniques were employed to characterize the plastic deformation zones around fatigue cracks in Fe–2.6 wt% Si. Both surface and sub-surface cross-sections are evaluated. The plastic zone size changes significantly in the surface layers. It is correlated with energy release rate, J, because of the elasto-plastic nature of crack propagation and a linear correlation is found. The plastic deformation experienced inside the plastic zone is analysed and is reported in terms of equivalent tensile strains. The material in the immediate vicinity of the crack tip experiences large plastic strains under a steep gradient. This region, however, occupies a very small fraction of the plastic zone, the rest of which is deformed to less than 4% plastic strain. In the light of the experimental data, an attempt is made to identify potential sources for the variation in measured plastic zone parameters reported in the literature.

1. Introduction

Most metals deform plastically before fracture. Consequently, the tip of a propagating fatigue crack is attended by a plastic deformation zone through which the crack extends. The energy available for crack extension is reduced by as much as that expended in the formation of a crack tip plastic zone (CTPZ). The constituents of these zones provide major energy sinks and ought to be taken into account for proper characterization of the resistance to crack propagation. Hence, an analysis of the CTPZ is necessary to understand the crack propagation behaviour of materials.

The deformability of the material at the crack tip has to be exhausted for crack extension to take place. A volume element starts experiencing irreversible deformation (both mechanically and thermodynamically) when it enters the plastic zone. Its deformation continues until the crack tip passes through or by it. Hence, energy is dissipated only inside the CTPZ, assuming that strain distribution in the specimen is uniform except around the crack tip. This dissipation can be estimated with a knowledge of plastic strain distribution within the plastic zone and the plastic flow behaviour of the material.

In addition to the strain distribution, the geometry (size and shape) of CTPZ is also of interest. Plastic zone size, r_p, is an important parameter. The energy dissipated within the plastic zone is proportional to the plastic zone size. The distance over which the yield strength of the material is exceeded at the crack tip is different in different directions. This results in various shapes. Therefore, for a complete geometrical characterization of the CTPZ, its shape ought to be known, as well. It should also be noted that plastic zone geometry arranges the distribution of residual stresses ahead of the crack tip and influences crack growth kinetics as demonstrated by overload experiments [1].

Various experimental techniques [2–18] have been used to study plastic zones. Some of these techniques are restricted to the surface of the specimen and can be used for the evaluation of the plane stress plastic zone only. On the other hand, those which can be applied on the interior cross-sections require the removal of deformed and roughened surface layers when the plane stress plastic zone is to be analysed. The depth of the material to be removed from the surface could be very large in the case of ductile materials, particularly when there is necking at the crack tip. As the plastic zone geometry changes through the thickness, particularly in the surface layers, characterization of surface plasticity has to be carried out prior to sectioning and/or grinding of surface layers for cross-sectional analysis. The change in plastic zone geometry in the surface layers could be significant unless the entire crack front experiences a plane stress state. Hence, for a comprehensive three-dimensional characterization of plastic zone geometry, a combination of the available techniques has to be employed. This is necessary also because of the limited resolution provided by the currently available techniques either in the high or low strain range. In the present study, surface roughness analysis, etch-pit, and recrystallization techniques were employed for the geometrical characterization of the CTPZ. An attempt was also made to evaluate the strain distribution around the crack tip.

2. Experimental procedures

An iron–silicon alloy with 2.6 wt% Si was used. Its yield strength and Young's modulus were 538 MPa and 207 GPa, respectively. The stress–strain curve for this alloy is shown in Fig. 1. Single-edge-notched (SEN) specimen geometry was used for fatigue crack propagation (FCP) tests. The specimens were machined

0022–2461/88 $03.00 + .12

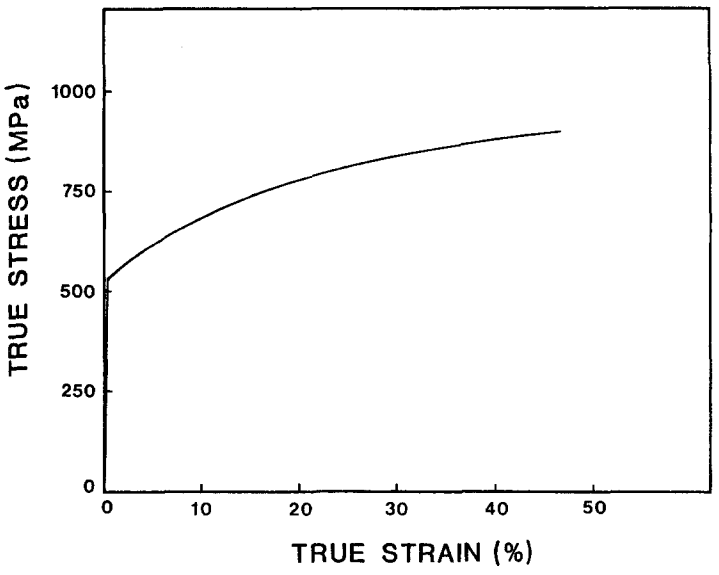

Figure 1 The stress–strain curve for Fe–2.6 wt % Si.

to obtain a length-to-width ratio of about 4. A 60° "V" notch of 1.5 mm depth was introduced at the middle of one edge of each specimen. For the range of crack propagation investigated, the thickness of the specimen (t) was smaller than the minimum thickness for plane strain conditions:

$$t < 2.5\,(K_{max}/\sigma_y)^2 \qquad (1)$$

where K_{max} and σ_y are the maximum stress intensity factor and yield strength of the material, respectively. The geometry of the FCP test specimens is illustrated in Fig. 2a.

The FCP tests were performed in laboratory atmosphere at room temperature with 20 kN capacity closed-loop servohydraulic MTS machine. The specimens were loaded in tension–tension with a sinusoidal wave form at a frequency of 5 Hz. The maximum load of the fatigue cycle was chosen as 40% of the yield strength of the present alloy. The minimum load was 10% of the maximum load (R = 0.1) and the load amplitude was kept constant throughout the crack propagation test. The loading conditions are summarized in Fig. 2b. The constant-load–amplitude fatigue tests provided increasing stress intensities with crack propagation and thus allowed the plastic zone characterization to be carried out at K_{max} values ranging from 20 to 60 MPa m$^{1/2}$.

As the initiation of a fatigue crack is usually time consuming even in the presence of a notch, higher maximum loads ($P_{max} = 0.6\,P_y$) and frequencies (10 Hz) were applied to accelerate the initiation process. The material in the vicinity of the notch always experiences plastic flow prior to the initiation of a crack. Hence, early crack propagation takes place through a deformation zone which is not characteristic of the crack itself. Therefore, the crack propagation and plastic zone evolution were evaluated starting from a crack length of about 0.5 mm.

Surface roughness, etch-pit, and recrystallization techniques were employed to characterize the plastic deformation zone around fatigue cracks. Calibration tests were carried out to correlate the response of the material to these techniques as a function of the plastic deformation it has experienced. This information is

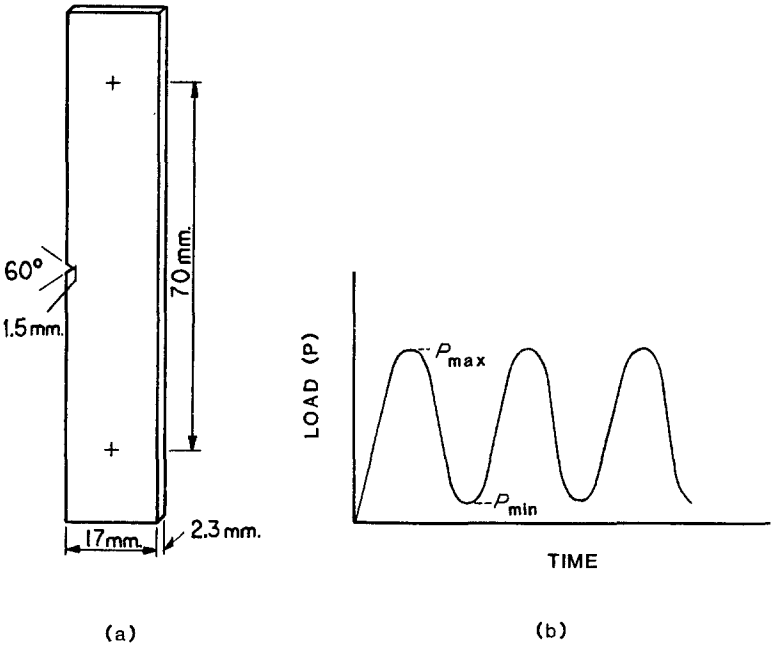

Figure 2 (a) The specimen geometry and (b) fatigue loading conditions: wave form = sine (tension–tension), frequency = 5 Hz, P_{max} = 0.6 P_y, 0.4 P_y (P_y = yield load), R = 0.1.

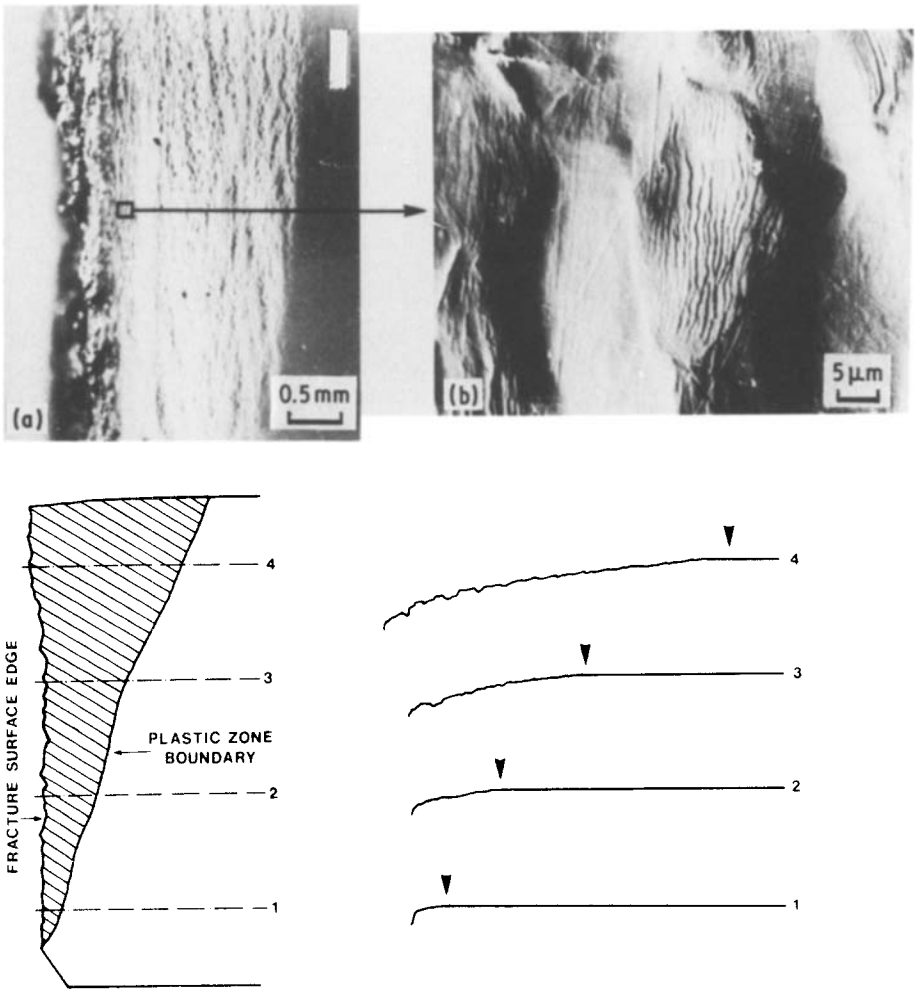

Figure 3 (a) Optical, (b) scanning electron micrographs of the surface deformation, and (c) application of profile analysis for its geometrical characterization.

needed to evaluate the strain distribution inside the crack tip plastic zones [19, 20]. Strips of Fe–2.6 wt % Si were deformed in tension to plastic strains ranging from 0.2% to 13%. This range covers the uniform straining region of the σ–ε curve. Calibration for higher strains ($\varepsilon_p > 15\%$) was carried out on necked portions of tensile specimens, the deformation of which was estimated from the analysis of cross-sectional area reduction. The necked regions have experienced plastic strains from about 15% at the start of necking to approximately 45% next to the fracture surface. Thus, the necked portion of a tensile specimen is expected to closely represent the immediate vicinity of a crack tip. Calibration information was used to assign each volume element within the plastic zone of a fatigue crack, an equivalent tensile strain.

Crack propagation and plastic zone evolution were monitored with a travelling microscope and were photographically recorded on a video tape using a camera attached to the microscope. The specimens were illuminated from different angles to establish dark-field conditions. Both the crack and the roughened surface layers were revealed very clearly under such conditions. Video observations, after the completion of the test, allowed frame-by-frame analysis of plastic zone evolution on the surface. Hence, geometrical characterization of the plane stress plastic zone was possible without the interruption of the test. Measurements from such observations were compared with optical microscopy and profile studies of side surfaces (Fig. 3) of fatigued specimens.

Following the surface roughness analysis, samples were carefully ground to remove the roughened surface layer and polished. Then, they were aged at 160° C for 45 min and electro-etched in Morris solution at 5 V for 30 to 45 min to allow selective pitting at sites where dislocations emerge at the surface to be examined. Ageing heat treatment brings about the segregation of interstitials to dislocations which enhances this kind of pitting, an example of which is illustrated in Fig. 4.

The etch-pit technique was selected because of its applicability on interior transverse and longitudinal cross-sections. This technique provides very good resolution at low strains, allowing the plastic zone boundary to be located precisely. Hence, it is very successful in geometrical characterization of plastic zones. Its resolution at high strains, however, is limited. Plastic strains larger than 4% could not be resolved.

The recrystallization technique was used to estimate the plastic strains in the immediate vicinity of the crack tip. The recrystallized grain size, however, does not change much with prior deformation at strains larger than 10 to 15%. Therefore, it is not possible to determine the crack tip strains, and the strain distribution close to the crack tip can only be roughly approximated [20].

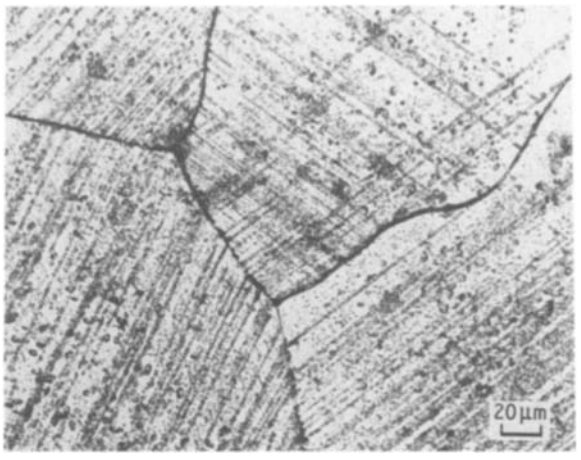

Figure 4 Distribution of etch-pits on the surface of a specimen deformed monotonically to 1%.

3. Results and discussion

A significant amount of plastic deformation accompanies fatigue crack propagation in Fe–2.6 wt % Si. The spread of this deformation on the surface is shown in Fig. 5. The roughening of an originally smooth surface is due to the different flow properties of neighbouring grains with different orientations and is referred to as the "orange peel" structure [21]. The extent of roughening is dictated by crack tip strain gradients and its density increases along the crack line with increasing crack length. Calibration tests have shown that the roughness develops on the surface of the specimen only when the yield strength of the material is exceeded. Hence, the plastic zone boundary can be located easily.

The extent of crack tip deformation is different along different directions. Hence, maximum plastic zone size, $r_{p,max}$, serves as a common dimensional characteristic of crack tip plasticity and is expressed by a fracture mechanics equation [22]:

$$r_{p,max} = \alpha(K_{max}/\sigma_y)^2 \quad (2)$$

This equation predicts large plastic zones for low yield-strength-materials and high stress-intensity conditions. α is a correlation coefficient which depends on the stress state and orientation relative to the crack propagation direction. Such a correlation for the Fe–Si alloy investigated in the present work, yields an α value of 0.3 for the surface (plane stress) plastic zone. This value agrees with the theoretical predictions [23, 24] and also falls within the range of measured α values [25–28]. However, it is quite unlikely that any measured α will be outside this range. The application of various experimental techniques in geometrical characterization of plastic zones have yielded significantly different values of α even for similar materials experiencing similar stress states. Values of α as high as 0.84 [27] and as small as 0.07 [28] have been reported for plane stress plastic zone. The former needs to be evaluated with caution as it was obtained for near-threshold conditions where plastic zone size was comparable to the grain size of the material.

Fig. 6 shows the plastic zone, revealed by the etch-pit technique, around the same fatigue crack as in Fig. 5 on a longitudinal cross-section at approximately 100 μm depth. Geometrical analysis of this zone indicates that the size of the CTPZ changes significantly in the surface layers. Plastic zone size is correlated with energy release rate due to the large scale of yielding at the crack tip (Fig. 7). The maximum energy release rate, J_{max}, is determined from evaluation of load against displacement curves recorded at different crack lengths during crack propagation. The following equations are obtained for plastic zone size at the surface and at 100 μm from

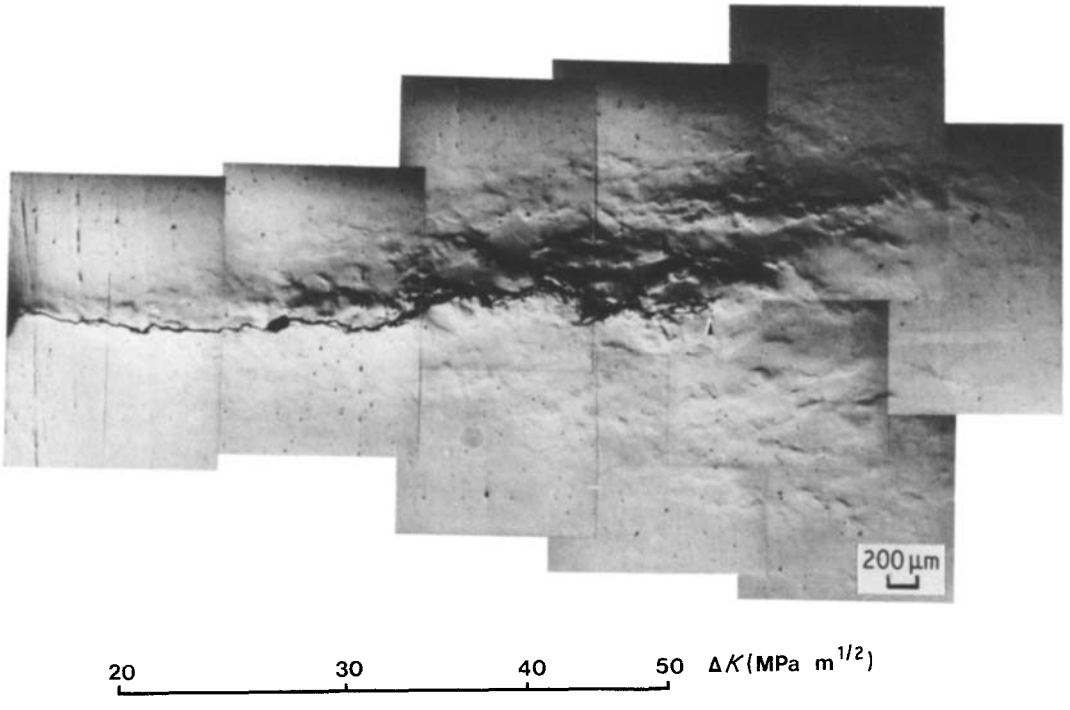

Figure 5 Surface deformation around a fatigue crack which was propagated under the following conditions: $P_{max} = 0.4\,P_y$ (P_y = yield load), $R = 0.1$, frequency = 5 Hz.

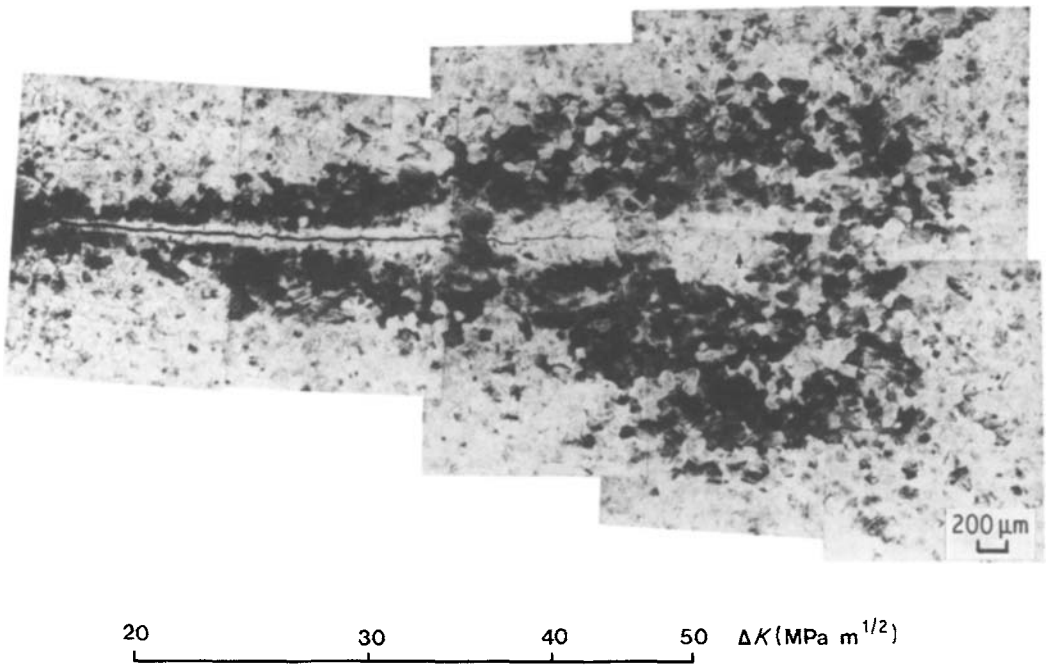

Figure 6 Plastic zone, revealed by the etch-pit technique, around the same fatigue crack as in Fig. 5, at 100 μm depth from the surface (marker indicates the crack tip).

the surface:

$$r_{p,max} = 0.39\ (E/\sigma_y^2)\ J_{max} \quad \text{(surface)} \qquad (3)$$

$$r_{p,max} = 0.21\ (E/\sigma_y^2)\ J_{max} \quad \text{(100 } \mu\text{m from the surface)} \qquad (4)$$

where E is the Young's modulus.

The plastic zone at the surface is almost twice as large as that at 100 μm depth. The latter is the outermost surface on which the etch-pit technique could be applied following the removal of the surface roughness. This pronounced change in size may be one of the factors contributing to the variation in measured α values reported in the literature for the plane stress plastic zones. Only those experimental techniques which are applicable directly to the free surface of a specimen provide information about the true plane stress plastic zone. While surface roughness analysis fits the above definition, etch-pit and other metallographic techniques do not, as they require the removal of roughened surface layers. The above explanation is not valid, however, in the case of plane strain plastic zone for which the range of measured values of α is noticeably smaller [25].

In addition to its size, the shape of the CTPZ also changes through the thickness. It becomes more and more circular away from the surface and remains more or less symmetrical with respect to the crack plane. The geometry change through the thickness is schematically illustrated in Fig. 8. The plastic zone shape in the surface layers is similar to that predicted by Tuba [29]. Various symmetrical [2, 30] and non-symmetrical [13] geometries were reported for CTPZs. The former is likely unless the plastic zone size is comparable to the microstructural characteristic dimension of the material. Weiss and Meyerson [13] argued that the geometry of the plastic zone is controlled by the local structural conditions, not by the crack tip stress field. Local instabilities were occasionally observed during crack propagation in Fe–2.6 wt % Si. These are believed to be due to the

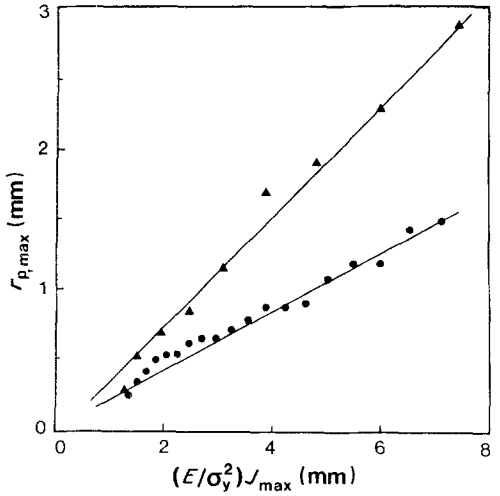

Figure 7 Variation of plastic zone size, $r_{p,max}$, with maximum energy release rate, J_{max}. (▲) Surface, (●) 100 μm from the surface.

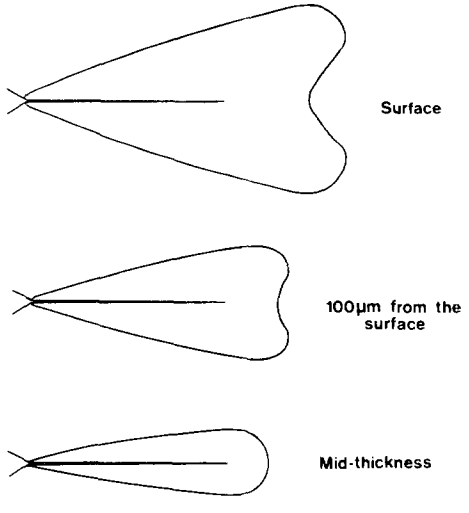

Figure 8 The change in plastic zone geometry through the thickness.

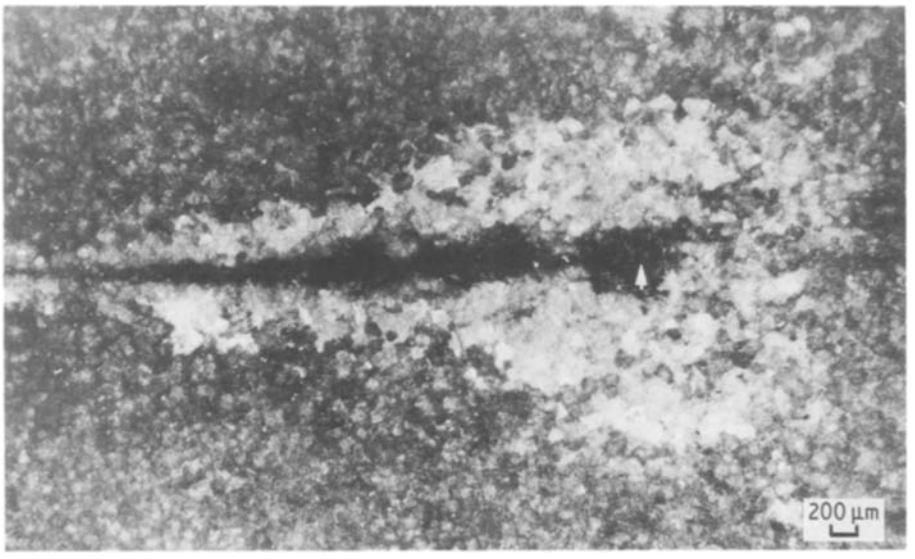

Figure 9 Dark-field micrograph of the etch-pit pattern around the fatigue crack shown in Fig. 6. Marker indicates the crack tip.

variation of ductility along the crack path and were correlated with evolutional characteristics of the plastic zone [19]. However, such instabilities affected only the immediate vicinity of the crack tip but did not change the overall geometry.

Observations of plastic zone evolution on the surface from video recordings indicate that the plastic zone does not have a particular geometry throughout the entire crack propagation life. The movement of the CTPZ, with increasing driving force, cannot be characterized in terms of translation and isotropic expansion, alone. The shape change of the CTPZ ought to be considered as well. A detailed analysis of plastic zone evolution is underway.

Two different regions can be seen inside the plastic zone in Fig. 6. The light etching region next to the crack has experienced plastic strains larger than 4%. This type of etching response is similar to that reported by Hahn *et al.* [31]. In their etch-pit studies of fatigued Fe–Si [2], they called this light etching region, the cyclic plastic zone, after Rice's prediction [23]. However, there is no experimental evidence indicating that the size of this zone at the crack tip, represents the extent of reversed plastic flow. Hence, the light etching zone in Fig. 6 will be referred to as the high strain zone (HSZ). The light appearance of this zone was attributed to an insufficiency of interstitials in solution [2]. It could also be due to the removal of an entire surface layer with etching as a result of a very high dislocation density. This would produce a flat surface effect. The latter explanation is supported by the dark-field micrograph of the etch-pit plastic zone (Fig. 9). The HSZ has a different contrast compared to the elastically deformed region outside the plastic zone.

The size of the HSZ is only about one-fifth of the plastic zone size, perpendicular to the crack propagation direction. However, its volume is estimated to be less than 5% of the entire CTPZ for the crack propagation range, investigated. This indicates that a very small portion of the plastic zone experiences plastic strains larger than 4% (Fig. 10). The rest of it is deformed to less than 4%, and appears dark in the etch-pit micrograph (Fig. 6). Another iso-strain contour can be located inside this outer zone (Fig. 11) with the information provided by the calibration studies. Between 2 and 4% plastic strain, the etched surface is merely dark due to the high density of etch

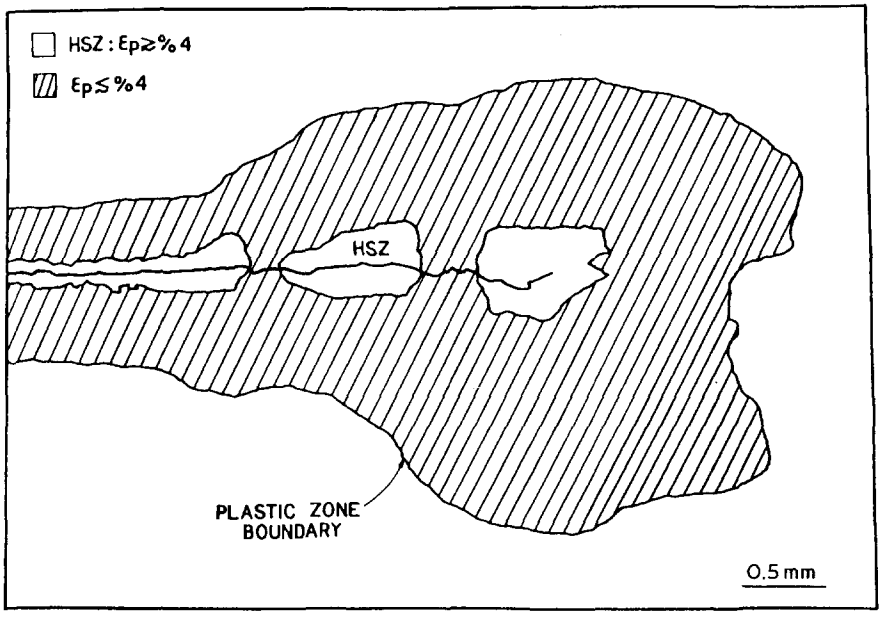

Figure 10 Distribution of plastic strain inside the plastic zone of the fatigue crack shown in Fig. 6.

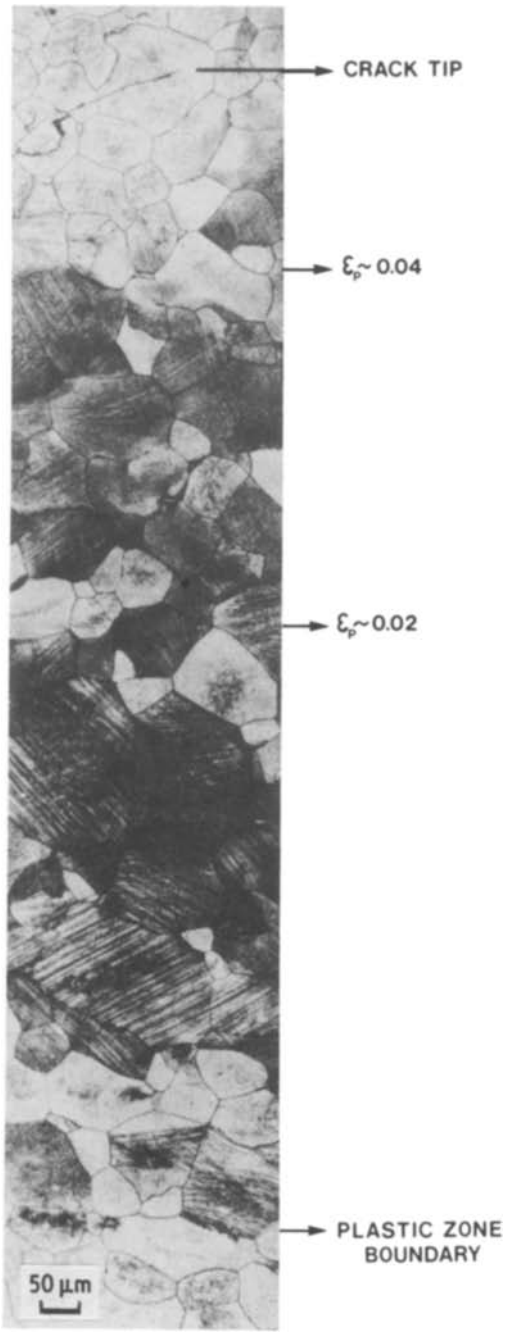

Figure 11 Analysis of strain distribution around the crack tip with the etch-pit technique.

pits. Individual dislocation etch pits and slip line configurations can be detected at plastic strains less than 2%.

As the etch-pit technique cannot resolve the strain distribution within the HSZ, an attempt was made to use the recrystallization technique for this purpose. The recrystallized grain size changes only about 50% from $\varepsilon_p = 10\%$ to $\varepsilon_p = 45\%$ at all annealing temperatures, investigated [20]. Hence, this technique proves to be more appropriate for geometrical characterization of plastic zones and supplies limited information in the high-strain range.

Fig. 12 illustrates the strain distribution around the crack tip. It is clear that the resolution provided by the experimental techniques is significant in plastic zone characterization. Some suffer drawbacks as they give limited or no information at high and/or low plastic

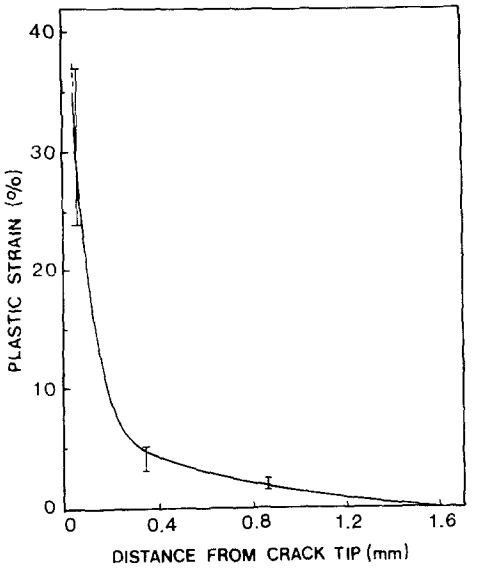

Figure 12 Variation of plastic strain at the crack tip, perpendicular to the crack propagation direction.

strains. For instance, a technique which has a minimum resolution of 2% plastic strain might underestimate the plastic zone size by one-half, when the strain distribution in Fig. 12 is considered. Very few of the available techniques can distinguish between small plastic and elastic strains for an accurate determination of the plastic zone boundary. Different sensitivities of different experimental techniques is believed to be one of the reasons for the variation in measured plastic zone parameters reported in the literature.

Strain distribution inside the plastic zone is not simply a function of crack tip stress field and yield strength of the material. Evaluation of crack tip strains for different materials, unlike CTPZ geometries, requires a consideration of strain hardening characteristics of these materials. It was shown theoretically [32] that the plastic zone size is not affected much by strain hardening behaviour.

4. Conclusions

The geometry of the plastic deformation zone and the strain distribution around fatigue cracks in Fe–2.6 wt % Si are evaluated. Both size and shape of the plastic zone change through the thickness, particularly in the surface layers. Hence, a three-dimensional analysis is necessary for a comprehensive characterization of plastic zones.

The change in plastic zone geometry through the thickness is believed to be partly responsible for the wide range of plastic zone parameters cited in the literature. Hence, a dimensionless parameter, d/t (d = depth from the surface; t = thickness of the sample), needs to be introduced in CTPZ characterization studies to validate comparisons.

The plastic deformation that accompanies crack propagation in Fe–2.6 wt % Si does not fall into the small-scale yielding category. Hence, plastic zone size, $r_{p,max}$, is correlated with the experimentally determined maximum energy release rate, J_{max}. A linear correlation is found.

Because of the nature of strain distribution around the crack tip, the plastic zone can be divided into two

regions. The strain gradients are very steep in the immediate vicinity of the crack tip. This region is referred to as the high strain zone (HSZ) and the 4% isostrain contour serves as its boundary. HSZ occupies a very small fraction of the CTPZ. The rest of the CTPZ experiences plastic strains smaller than 4%. Most experimental techniques employed in CTPZ analysis have limited resolution at low strains and could underestimate the plastic zone size.

The crack tip strain is dictated by the deformability of the material at the crack tip which has to be exhausted for crack extension to take place. It can be very large for ductile materials. The resolutional power of the currently available techniques, however, is limited at about 20% plastic strain. The recrystallization technique provides some insight into the magnitude of strains in the HSZ. The spatial resolution of this technique has to be improved, however, by making the grain size of the material as small as possible.

References

1. J. LANKFORD and D. L. DAVIDSON, *J. Eng. Mater. Technol.* **98** (1976) 17.
2. G. T. HAHN, R. G. HOAGLAND and A. R. ROSENFIELD, *Metall. Trans.* **3** (1972) 1189.
3. C. BATHIAS and R. M. PELLOUX, *ibid.* **4** (1973) 1265.
4. M. CLAVEL, D. FOURNIER and A. PINEAU, *ibid.* **6A** (1975) 2305.
5. G. CHALANT and L. REMY, *Mater. Sci. Engng* **50** (1981) 253.
6. Y. IINO, *Met. Sci.* **12** (1978) 207.
7. E. HORNBOGEN, E. MINUTH and ST. STANZL, *Mater. Sci. Engng* **43** (1980) 145.
8. E. TSCHEGG, C. FALTIN and S. STANZL, *J. Mater. Sci.* **15** (1980) 131.
9. J. S. CROMPTON and J. W. MARTIN, *Mater. Sci. Engng* **64** (1984) 37.
10. D. L. DAVIDSON and J. LANKFORD, *J. Eng. Mater. Technol.* **98** (1976) 24.
11. D. L. DAVIDSON, J. LANKFORD, T. YOKOBORI and K. SATO, *Int. J. Fract.* **12** (1976) 579.
12. M. A. WILKINS and G. C. SMITH, *Acta Metall.* **18** (1970) 1035.
13. B. Z. WEISS and M. R. MEYERSON, *Eng. Fract. Mech.* **3** (1971) 475.
14. D. R. WILLIAMS, D. L. DAVIDSON and J. LANKFORD, *Exp. Mech.* **20** (1980) 134.
15. W. J. BAXTER and S. R. ROUZE, *Met. Trans.* **7A** (1976) 647.
16. T. D. DUDDERAR, *Exp. Mech.* **9** (1969) 281.
17. S. I. KWUM and M. E. FINE, *Scripta Metall.* **14** (1980) 155.
18. A. OHTA, M. KOSUGE and E. SASAKI, *Int. J. Fract.* **13** (1977) 289.
19. Y. BIROL, *Metallography* **21** (1988) 77.
20. *Idem, J. Mater. Sci. Lett.* **6** (1987) 1161.
21. "Metals Handbook", 9th Edn., Vol. 9 (ASM, Ohio, 1985) p. 687.
22. D. BROEK, "Elementary Engineering Fracture Mechanics" (Noordhoff, The Netherlands, 1984) p. 91.
23. J. R. RICE, STP 415 (American Society for Testing and Materials, Philadelphia, 1967) p. 247.
24. D. S. DUGDALE, *J. Mech. Phys. Solids* **8** (1960) 100.
25. J. LANKFORD, D. L. DAVIDSON and T. S. COOK, STP 637 (American Society for Testing and Materials, Philadelphia, 1977) p. 36.
26. J. LANKFORD and D. L. DAVIDSON, *Int. J. Fract.* **14** (1978) R87.
27. K. TANAKA, M. HOJO and Y. NAKAI, *Mater. Sci. Engng* **55** (1982) 85.
28. T. YOKOBORI, K. SATO and H. YAGUCHI, *Rep. Res. Inst. Strength and Fract. Mater. Tohoku Univ.* **9** (1973) 1.
29. I. S. TUBA, *J. Strain Anal.* **1** (1966) 115.
30. Y. WAKU, T. MASUMOTO and T. OGURA, *Trans. Jpn Inst. Metals* **24** (1983) 849.
31. G. T. HAHN, P. N. MINCER and A. R. ROSENFIELD, *Exp. Mech.* **11** (1971) 248.
32. D. M. TRACEY, *J. Engng Mater. Technol.* **98** (1976) 146.

Received 14 May
and accepted 22 September 1987